AD-A139 042 CORROSION AND LOAD TRANSFER EFFECTS ON FATIGUE OF 1/1
MECHANICALLY FASTENED J..(U) NAVAL AIR DEVELOPMENT
CENTER WARMINSTER PA AIRCRAFT AND CREW S.. E U LEE
UNCLASSIFIED 04 OCT 83 NADC-83133-60 F/G 13/5 NL

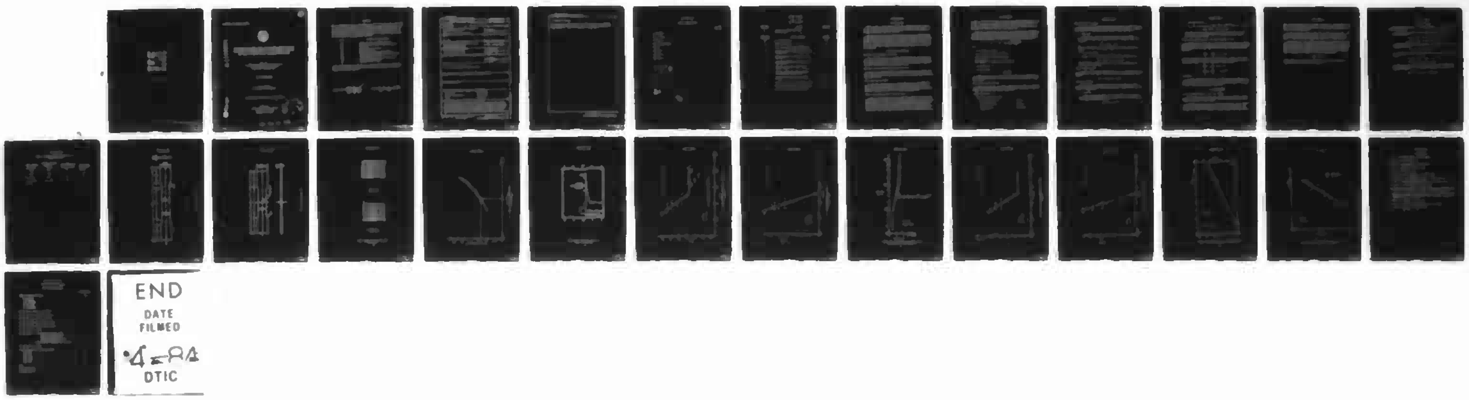

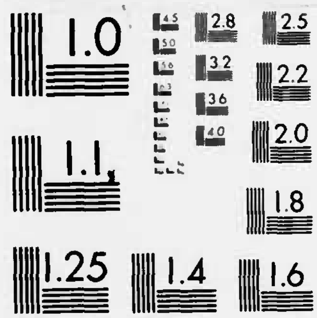

MICROCOPY RESOLUTION TEST CHART
NATIONAL BUREAU OF STANDARDS-1963-A

(12)

REPORT NO. NADC-83133-60

AD A139042

CORROSION AND LOAD TRANSFER EFFECTS ON FATIGUE OF MECHANICALLY FASTENED JOINTS
FATIGUE OF ZERO LOAD TRANSFER SPECIMEN

E. U. Lee
Aircraft and Crew Systems Technology Directorate
NAVAL AIR DEVELOPMENT CENTER
Warminster, Pennsylvania 18974

4 OCTOBER 1983

PHASE REPORT
Work Unit No. GC128/ZR00001

Approved For Public Release; Distribution Unlimited

DTIC FILE COPY

DTIC
SELECTE
MAR 1 6 1984
D
E

Prepared For
NAVAL AIR SYSTEMS COMMAND
Department of the Navy
Washington, DC 20361

84 03 15 005

NOTICES

REPORT NUMBERING SYSTEM – The numbering of technical project reports issued by the Naval Air Development Center is arranged for specific identification purposes. Each number consists of the Center acronym, the calendar year in which the number was assigned, the sequence number of the report within the specific calendar year, and the official 2-digit correspondence code of the Command Office or the Functional Directorate responsible for the report. For example: Report No. NADC-78015-20 indicates the fifteenth Center report for the year 1978, and prepared by the Systems Directorate. The numerical codes are as follows:

CODE	OFFICE OR DIRECTORATE
00	Commander, Naval Air Development Center
01	Technical Director, Naval Air Development Center
02	Comptroller
10	Directorate Command Projects
20	Systems Directorate
30	Sensors & Avionics Technology Directorate
40	Communication & Navigation Technology Directorate
50	Software Computer Directorate
60	Aircraft & Crew Systems Technology Directorate
70	Planning Assessment Resources
80	Engineering Support Group

PRODUCT ENDORSEMENT – The discussion or instructions concerning commercial products herein do not constitute an endorsement by the Government nor do they convey or imply the license or right to use such products.

APPROVED BY: W. J. Gallagher DATE: 30 January 1984

W. J. GALLAGHER
CAPT, MSC, USN

UNCLASSIFIED
SECURITY CLASSIFICATION OF THIS PAGE (When Data Entered)

REPORT DOCUMENTATION PAGE		READ INSTRUCTIONS BEFORE COMPLETING FORM
1. REPORT NUMBER NADC-83133-60	2. GOVT ACCESSION NO. AD A139 042	3. RECIPIENT'S CATALOG NUMBER
4. TITLE (and Subtitle) Corrosion and Load Transfer Effects on Fatigue of Mechanically Fastened Joints Fatigue of Zero Load Transfer Specimen		5. TYPE OF REPORT & PERIOD COVERED Phase Report 6. PERFORMING ORG. REPORT NUMBER
7. AUTHOR(s) E. U. Lee		8. CONTRACT OR GRANT NUMBER(s)
9. PERFORMING ORGANIZATION NAME AND ADDRESS Aircraft and Crew System Technology Directorate Naval Air Development Center Warminster, Pennsylvania 18974		10. PROGRAM ELEMENT, PROJECT, TASK AREA & WORK UNIT NUMBERS Work Unit GC128/ZR00001
11. CONTROLLING OFFICE NAME AND ADDRESS Naval Air Development Center Warminster, Pennsylvania 18974		12. REPORT DATE 4 October 1983 13. NUMBER OF PAGES 24
14. MONITORING AGENCY NAME & ADDRESS(if different from Controlling Office)		15. SECURITY CLASS. (of this report) Unclassified 15a. DECLASSIFICATION/DOWNGRADING SCHEDULE

16. DISTRIBUTION STATEMENT (of this Report)

Approved for Public Release; Distribution Unlimited

17. DISTRIBUTION STATEMENT (of the abstract entered in Block 20, if different from Report)

18. SUPPLEMENTARY NOTES

19. KEY WORDS (Continue on reverse side if necessary and identify by block number)

Load Transfer	Crack Initiation
Mechanically Fastened Joint	Crack Growth
Fatigue	Stress Range

20. ABSTRACT (Continue on reverse side if necessary and identify by block number)

This IR program studies the effects of load transfer and corrosive environment on fatigue of mechanically fastened joints. As an initial part of the program, the fatigue crack initiation and growth, and the final fracture in zero load transfer specimens of 7475-T7351 aluminum alloy were investigated. The applied stress range $\Delta\sigma$ was related to the fatigue crack initiation life N_i and the total fatigue life N_f by empirical equations of the forms $\log N = a - b\,\Delta\sigma$ and $\log N = a - b\,(\Delta\sigma - \Delta\sigma_{th})$. The variation of fatigue crack growth rate with stress intensity factor

DD FORM 1 JAN 73 1473 EDITION OF 1 NOV 65 IS OBSOLETE
S/N 0102-LF-014-6601

UNCLASSIFIED
SECURITY CLASSIFICATION OF THIS PAGE (When Data Entered)

20. ABSTRACT (continued)

range was defined by $da/dN = (5.45 \times 10^{-9}) \cdot (\Delta K)^{2.94}$. The proportion of fatigue crack initiation and growth lives was determined as a function of the stress range and the total fatigue life: $N_i/N_f = 1 - N_p/N_f = 1.73 - 0.04\,\Delta\sigma = 1 - 245\,N_f^{-0.63}$

TABLE OF CONTENTS

Accession For
NTIS GRA&I ☒
DTIC TAB ☐
Unannounced ☐
Justification
By
Distribution/
Availability Codes
Dist | Avail and/or Special
A-1

LIST OF TABLES

LIST OF FIGURES

INTRODUCTION

Mechanically fastened joints facilitate ready assembly and disassembly of structural parts for construction, maintenance, repair, and replacement. They significantly affect both fabrication cost and structural reliability in aircraft. Most importantly, however, mechanically fastened joints are a principal source of aircraft structural failures in service.

Where varying loads are applied, the mechanically fastened joints become particularly susceptible to fatigue cracking. Such fatigue cracking is influenced greatly by load transfer through fasteners and aggravated by a corrosive environment. To understand the effect of load transfer, the baseline knowledge on the fatigue cracking, unaffected by any load transfer, is essential. This part of the IR program aims to characterize the phenomenon of fatigue cracking in a zero load transfer specimen. Employing a dogbone specimen, which has an open-hole simulating a fastener-hole at the center and is free of any load transfer, the behaviors of fatigue crack initiation and growth, and final fracture were investigated.

EXPERIMENTAL PROCEDURE

MATERIAL AND SPECIMEN PREPARATION

Since 7475-T7351 aluminum alloy is increasingly used for aircraft structural components, its plate, 1/4 in. thick, was selected as the specimen material. Dogbone specimens were prepared from the plate to have the longitudinal axis in the original plate drawing direction, figure 1. The specimen for fatigue test has an open-hole of 1/4 in. dia. at the center, figure 2; whereas, that for tensile test has no hole. The specimen hole was made by drilling and reaming.

DETERMINATION OF STRESS CONCENTRATION FACTOR

By employing the photoelasticity method, the elastic strains and stresses were measured along the horizontal axis in a dogbone specimen with an open-hole at the center under a vertical tension. With those elastic stresses and the gross stress of the specimen, the corresponding stress concentration factors were determined.

TENSILE AND FATIGUE TESTS

Both the tensile and fatigue tests were done on a closed-loop electro-hydraulic 90563 MTS system in a controlled laboratory atmosphere of 75°F and 45% relative humidity. The tensile test was performed, using dogbone specimens, at loading rate of 50,000 psi/min. The fatigue test was executed, using open-hole dogbone specimens, under constant amplitude loading of a haversine waveform with a stress ratio ($\sigma_{min}/\sigma_{max}$) of R = 0.05 and a frequency of 10 Hz.

DETECTION AND MEASUREMENT OF FATIGUE CRACK

Fatigue cycling was stopped at various loading intervals, and the specimen hole was inspected with a MAGNAFLUX HT-100 Eddy Current Hole Scanner for a possible crack initiation. Any crack presence is indicated by a group of eddy current signal spikes, whose heights are proportional to the depths at several crack front points, figure 3. The greatest height of the eddy current signal spikes was converted to the crack depth by comparing with the data from EDM (Electrical Discharge Machining) notches of known depths, 0.008, 0.015, 0.030, and 0.060 in. in a geometrically similar calibration standard of the same material. The determined crack depth was plotted against the corresponding number of loading cycles, and a crack growth curve was established. From this curve,

the particular number of loading cycles to produce a 0.01 in. deep crack was taken and defined as the fatigue crack initiation life in this study, figure 4. (Though the Eddy Current Hole Scanner is capable of finding smaller cracks, e.g. 0.005 in. deep cracks, it can detect 0.01 in. deep cracks more accurately and reliably. Other investigators [1,2] also defined the number of loading cycles required to produce a 0.01 in. deep crack as the fatigue crack initiation life.)

When the crack became visible on the specimen surface, the cyclic loading was stopped and the crack length was measured visually using a traveling microscope. This measurement was repeated until the crack tip reached an edge of the specimen or the specimen was fractured. Then the rate of crack growth da/dN was determined. The corresponding stress intensity factor range ΔK was calculated for a single crack emanating from the open-hole, employing the following equations[3–6].

$$\Delta K = \Delta\sigma \sqrt{\pi a} \cdot F_1(a/r) \cdot \sqrt{\sec\left\{\frac{\pi(a+2r)}{2W}\right\}} \tag{1}$$

where

$\Delta\sigma$: stress range, $(\sigma_{max} - \sigma_{min})$

a: length of crack emanating from open-hole

$F_1(a/r)$: Bowie factor for single hole-edge crack

$\sqrt{\sec\left\{\frac{\pi(a+2r)}{2W}\right\}}$: correction factor for specimen width

r: radius of open-hole

W: specimen width

RESULTS

The results are divided into six parts: stress concentration factor, tensile properties, fatigue crack initiation, fatigue crack growth, fatigue fracture, and proportion of fatigue crack initiation and growth lives.

STRESS CONCENTRATION FACTOR

The determined stress concentration factor K_t decreases with the distance from the hole edge, drastically in its immediate vicinity, along the horizontal axis, figure 5. The maximum stress concentration factor occurs at the hole edge and its value is 3.12.

TENSILE PROPERTIES

The result of tensile test is as follows:

yield stress (0.2% offset):	64.5 ksi
ultimate tensile stress:	73.5 ksi
elastic modulus:	9.7×10^3 ksi

FATIGUE CRACK INITIATION

From the results of fatigue test and crack inspection, the relationship of applied stress range $\Delta\sigma$ and fatigue crack initiation life N_i can be described by two different plots of $\Delta\sigma$ vs. log N_i and $(\Delta\sigma - \Delta\sigma_{th})$ vs. log N_i. ($\Delta\sigma_{th}$ is the threshold stress range for fatigue crack initiation.)

a. $\Delta\sigma$ vs. log N_i

The plot of $\Delta\sigma$ vs. log N_i has the feature of a typical S–N curve with a knee at $\Delta\sigma_{th}$ = 17.2 ksi, figure 6. For $\Delta\sigma > \Delta\sigma_{th}$, the plot results in a straight line, defined by the equation

$$\log N_i = 8.51 - 0.17\,\Delta\sigma \tag{2}$$

Below $\Delta\sigma_{th}$, no detectable crack was initiated within the limit number of loading cycles employed.

b. $(\Delta\sigma - \Delta\sigma_{th})$ vs. log N_i

The plot of $(\Delta\sigma - \Delta\sigma_{th})$ vs. log N_i is a straight line, figure 7, defined by the equation

$$\log N_i = 5.63 - 0.17\,(\Delta\sigma - \Delta\sigma_{th}) \tag{3}$$

Its intercept 5.63 is less than and its slope – 0.17 is identical to the corresponding value of $\Delta\sigma$ vs. log N_i plot for $\Delta\sigma > \Delta\sigma_{th}$.

FATIGUE CRACK GROWTH

The variation of fatigue crack growth rate da/dN with stress intensity factor range ΔK follows a sigmoidal curve, as shown in figure 8. The log-linear portion of the curve takes a form of Paris' equation[6]

$$da/dN = (5.45 \times 10^{-9}) \cdot (\Delta K)^{2.94} \tag{4}$$

FATIGUE FRACTURE

The fatigue fracture life or total fatigue life N_f, the number of fatigue loading cycles to fracture, can be represented as a function of stress range $\Delta\sigma$ by two different curves of $\Delta\sigma$ vs. log N_f and $(\Delta\sigma - \Delta\sigma_{th})$ vs. log N_f.

a. $\Delta\sigma$ vs. log N_f

The curve of $\Delta\sigma$ vs. log N_f has a form similar to a typical S-N curve and the curve of $\Delta\sigma$ vs. log N_i, and it has a knee at $\Delta\sigma_{th}$ = 17.2 ksi, figure 9. For $\Delta\sigma > \Delta\sigma_{th}$, the data can be fit in a straight line defined by the equation

$$\log N_f = 8.19 - 0.15\,\Delta\sigma \tag{5}$$

b. $(\Delta\sigma - \Delta\sigma_{th})$ vs. log N_f

The curve of $(\Delta\sigma - \Delta\sigma_{th})$ vs. log N_f is a straight line, figure 10, defined by the equation

$$\log N_f = 5.64 - 0.15\,(\Delta\sigma - \Delta\sigma_{th}) \tag{6}$$

Its intercept 5.64 is less than and its slope −0.15 is identical to the corresponding value of $\Delta\sigma$ vs. log N_f curve for $\Delta\sigma > \Delta\sigma_{th}$. Furthermore, the intercept 5.64 is close to that of $(\Delta\sigma - \Delta\sigma_{th})$ vs. log N_i curve 5.63.

PROPORTION OF FATIGUE CRACK INITIATION AND GROWTH LIVES

The fraction of total fatigue life spent for crack initiation or the ratio of fatigue crack initiation life to total fatigue life, N_i/N_f, was found to vary between 0.61 and 0.91, increasing with decreasing stress range. The reverse is true for the fatigue crack growth life N_p. The variation is delineated by a plot of $\Delta\sigma$ vs. N_i/N_f or $\Delta\sigma$ vs. N_p/N_f, figure 11. This plot is a straight line and can be defined by the equation

$$\frac{N_i}{N_f} = 1 - \frac{N_p}{N_f} = 1.73 - 0.04\,\Delta\sigma \tag{7}$$

The ratio of fatigue crack growth life to total fatigue life N_p/N_f or $(1 - N_i/N_f)$ was noticed to decrease with increasing total fatigue life N_f. This variation is shown by a plot of N_p/N_f vs. N_f on log-log coordinates in figure 12. This plot is a straight line defined by the equation

$$\frac{N_p}{N_f} = 1 - \frac{N_i}{N_f} = 245\,N_f^{-0.63} \tag{8}$$

or

$$\frac{N_i}{N_f} = 1 - \frac{N_p}{N_f} = 1 - 245\,N_f^{-0.63} \tag{9}$$

DISCUSSION

The determined stress concentration factor $K_t = 3.12$ at the hole edge in the employed specimen of width w = 1.50 in. and hole diameter d = 0.25 in. is in agreement with those reported by others.[7,8] Howland's curve[7] of K_t vs. d/w indicates $K_t = 3.095$ for a specimen of w = 1.50 in. and d = 0.25 in. Employing the Heywood's empirical equation[8],

$$K_t = \frac{2 + (1 - d/w)^3}{(1 - d/w)} \tag{10}$$

K_t is calculated to be 3.094 for w = 1.50 in. and d = 0.25 in.

The measured values of yield stress (64.5 ksi), ultimate tensile stress (73.5 ksi), and elastic modulus (9.7×10^3 ksi) of the specimen material, 7475-T7351 aluminum alloy, are close to and confirm those reported by others[9–11], table I.

In this study, two different plots of $\Delta\sigma$ vs. log N_i (or log N_f) and $(\Delta\sigma - \Delta\sigma_{th})$ vs. log N_i (or log N_f) were employed to relate the applied stress range $\Delta\sigma$ with the fatigue crack initiation life N_i or the total fatigue life N_f. The plot of $\Delta\sigma$ vs. log N_i (or log N_f) represents the overall variation of N_i (or N_f) with $\Delta\sigma$ and delineates a threshold stress range for fatigue crack initiation

$\Delta\sigma_{th}$, if it exists. The $\Delta\sigma_{th}$ is equivalent to the fatigue limit in a typical S–N curve. Foreman[1] and Wetzel[12] also employed this semi-long plot, but Allery and Birkbeck[13] preferred a log-log plot. The plot of $(\Delta\sigma - \Delta\sigma_{th})$ vs. log N_i (or log N_f) reflects the influence of $\Delta\sigma_{th}$ on the fatigue crack initiation life N_i (or the total fatigue life N_f).

The fatigue crack growth rate $da/dN = (5.45 \times 10^{-9}) \cdot (\Delta K)^{2.94}$, found in this study, is close to that determined by Margolis[11], $da/dN = (2.13 \times 10^{-9}) \cdot (\Delta K)^{3.51}$. To obtain this result, Margolis[11] fatigue-tested compact tension specimens under constant amplitude loading of stress ratio $R = 0.5$, stress intensity factor range $\Delta K < 26$ ksi, and frequency $f = 360$ cpm in dry air.

As indicated by $N_i/N_f = 0.61 \sim 0.99$ within the limits of $\Delta\sigma$ value employed, the fatigue crack initiation occurs quite late in the total fatigue life, and the smaller the $\Delta\sigma$ value, the longer is the fatigue crack initiation stage. A similar observation was also made by Manson[14] in the fatigue study of 410 stainless steel, 4130 steel, 2024-T4 aluminum alloy, pure aluminum, pure nickel, and polycarbonate resin. Especially, in the case of polycarbonate resin, the initiation of a crack, 0.002 to 0.003 in. deep, occurred at approximately 65% of the total fatigue life for the low cycle test and 85% for the high cycle test. He related N_i and N_f with the following equation

$$1 - \frac{N_i}{N_f} = 2.5\, N_f^{-1/3} \tag{11}$$

The numerical factors in this equation, the intercept and slope of log-log plot, are different from those of equation 8, which was formulated in this study.

CONCLUSIONS

From this fatigue study with the zero load transfer specimen of 7475-T7351 aluminum alloy, the following is concluded.

1. The fatigue crack initiation life N_i can be related to the applied stress range $\Delta\sigma$ by the following two equations

$$\text{(a)}\quad \log N_i = 8.51 - 0.17\,\Delta\sigma \qquad \text{for } \Delta\sigma > \Delta\sigma_{th}$$

$$\text{(b)}\quad \log N_i = 5.63 - 0.17\,(\Delta\sigma - \Delta\sigma_{th})$$

2. The variation of fatigue crack growth rate da/dN with stress intensity factor range ΔK is defined by the equation

$$da/dN = (5.45 \times 10^{-9}) \cdot (\Delta K)^{2.94}$$

3. The total fatigue life N_f can be related to the applied stress range $\Delta\sigma$ by the following two equations

$$\text{(a)}\quad \log N_f = 8.19 - 0.15\,\Delta\sigma \qquad \text{for } \Delta\sigma > \Delta\sigma_{th}$$

$$\text{(b)}\quad \log N_f = 5.64 - 0.15\,(\Delta\sigma - \Delta\sigma_{th})$$

4. The crack initiation portion of the total fatigue life, N_i/N_f, is greater than 60% within the employed stress range limits, and it increases with decreasing $\Delta\sigma$ and increasing N_f, as indicated by the equation

$$\frac{N_i}{N_f} = 1.73 - 0.04\,\Delta\sigma = 1 - 245\,N_f^{-0.63}$$

TABLE I. MECHANICAL PROPERTIES OF 7475-T7351 ALUMINUM ALLOY

YIELD STRESS σ_{ys}, (ksi)	ULTIMATE TENSILE STRESS σ_{tu} (ksi)	ELASTIC MODULUS E, (ksi x 10^3)	REFERENCE
64.5	73.5	9.7	this study
64.0	74.0	–	9
62.0	70.2	10.4	10
60.6 – 62.0	71.6 – 72.8	11.0	11

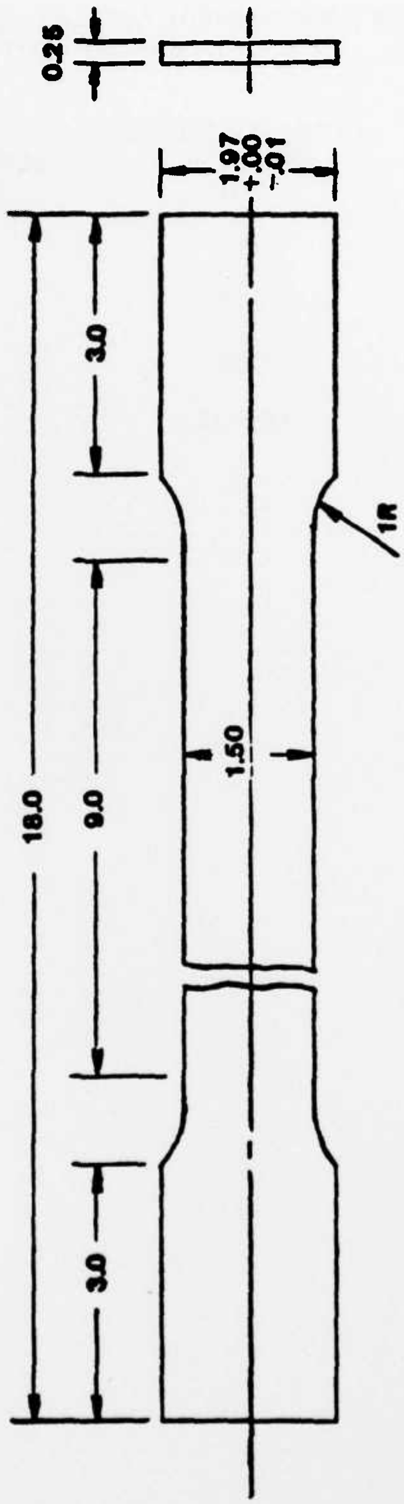

Figure 1. Tensile Test Specimen

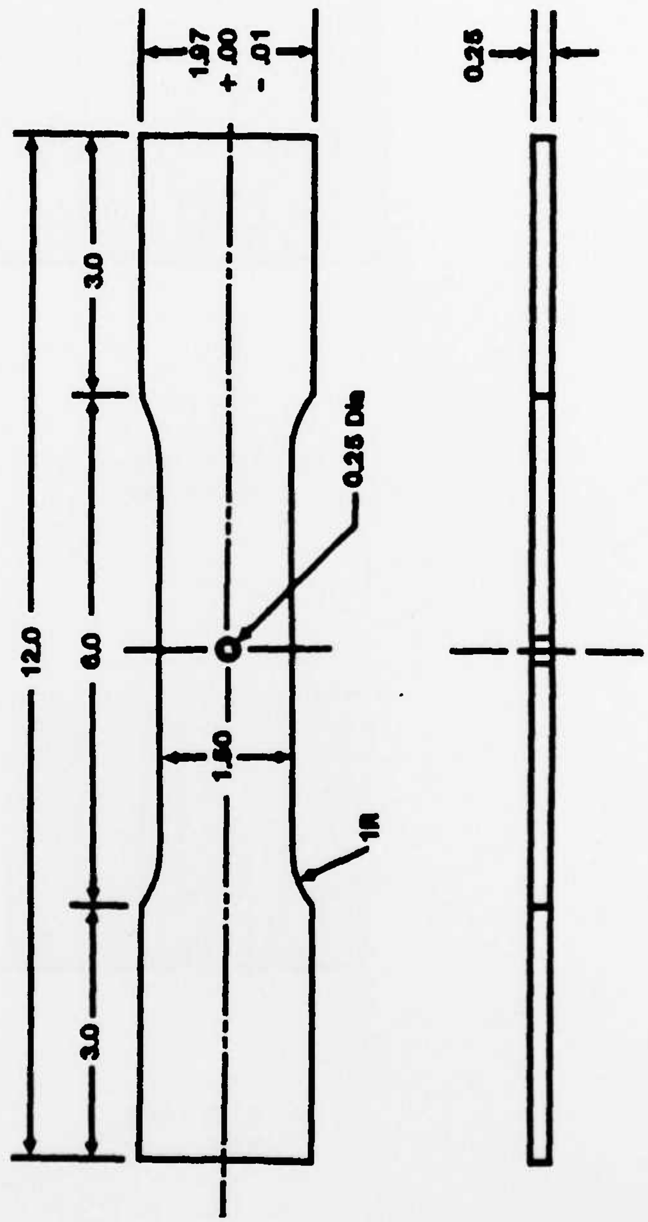

Figure 2. Fatigue Test Specimen

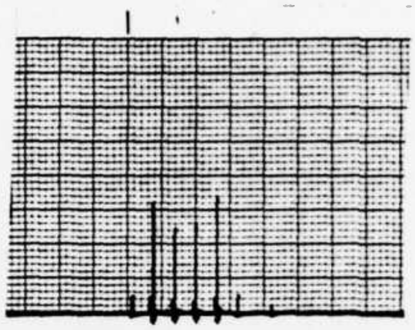

(a) 0.060 in. long
0.030 in. deep

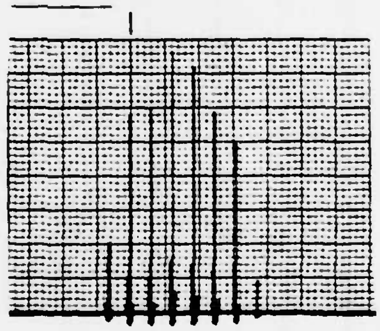

(b) 0.120 in. long
0.060 in. deep

Figure 3. Eddy Current Signal Spikes from EDM Notches

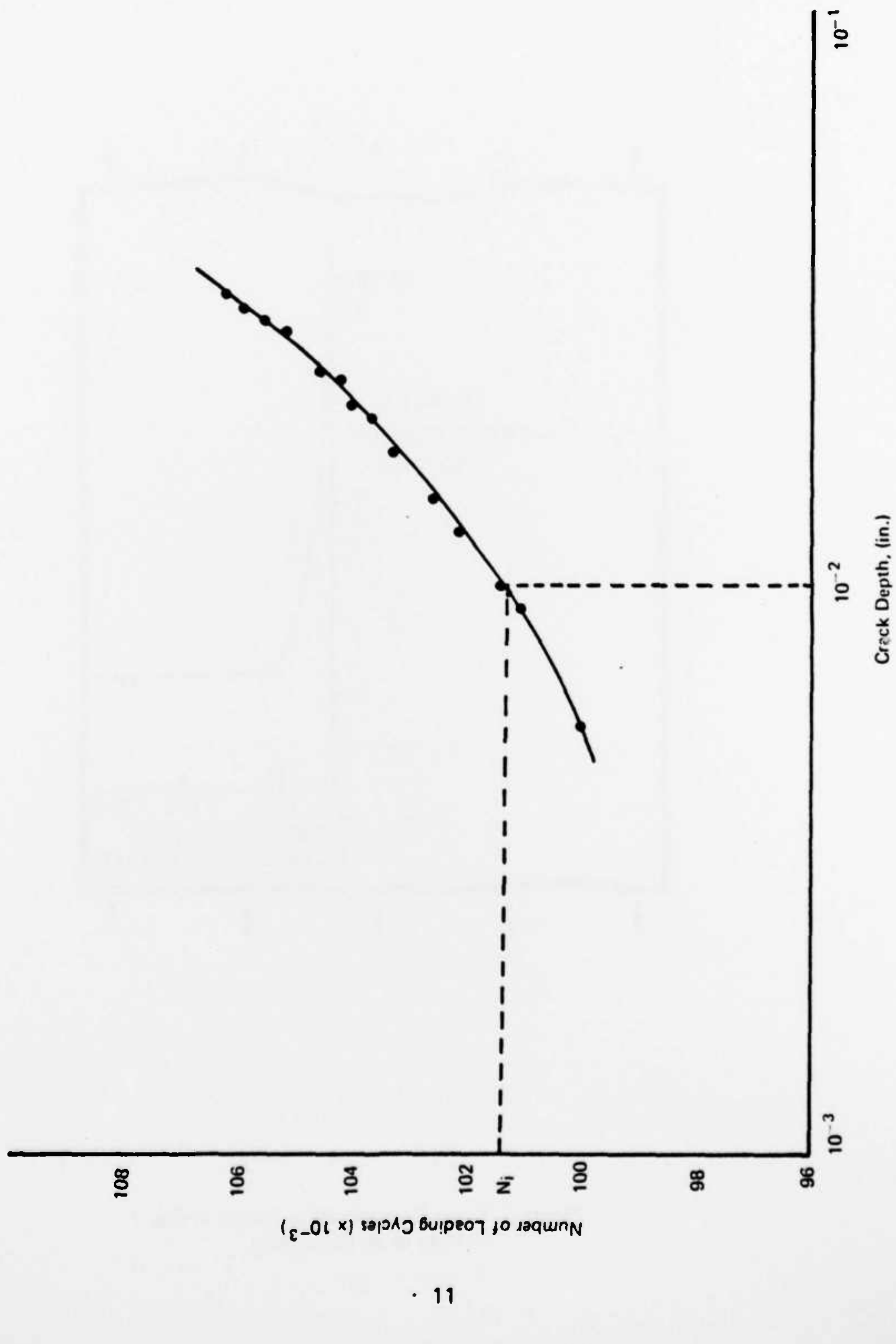

Figure 4. Crack Growth Curve Established with Eddy Current Inspection Result

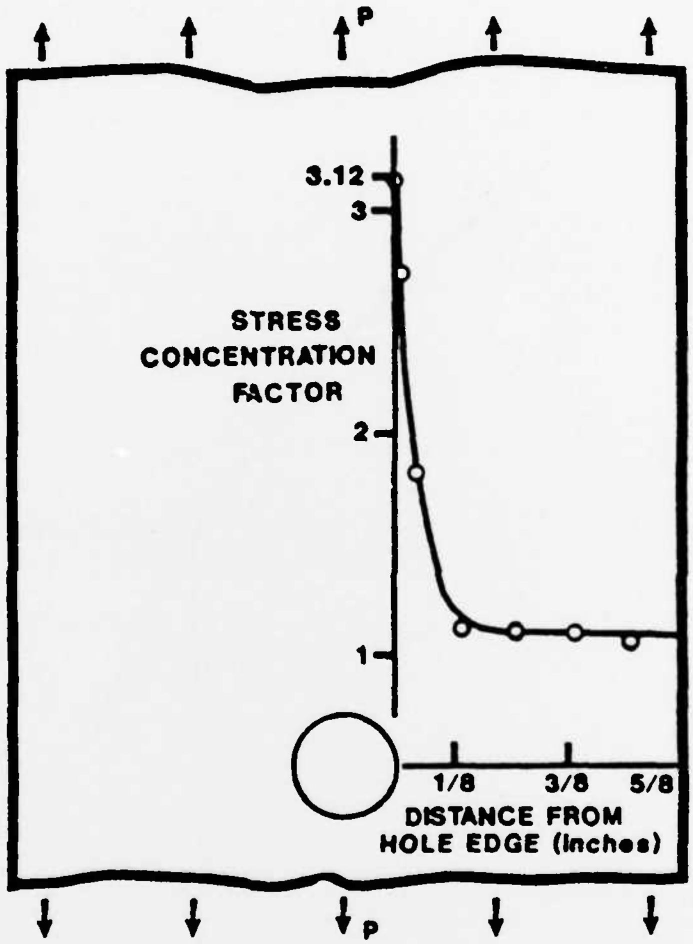

Figure 5. Stress Concentration Factor in the Vicinity of an Open-Hole

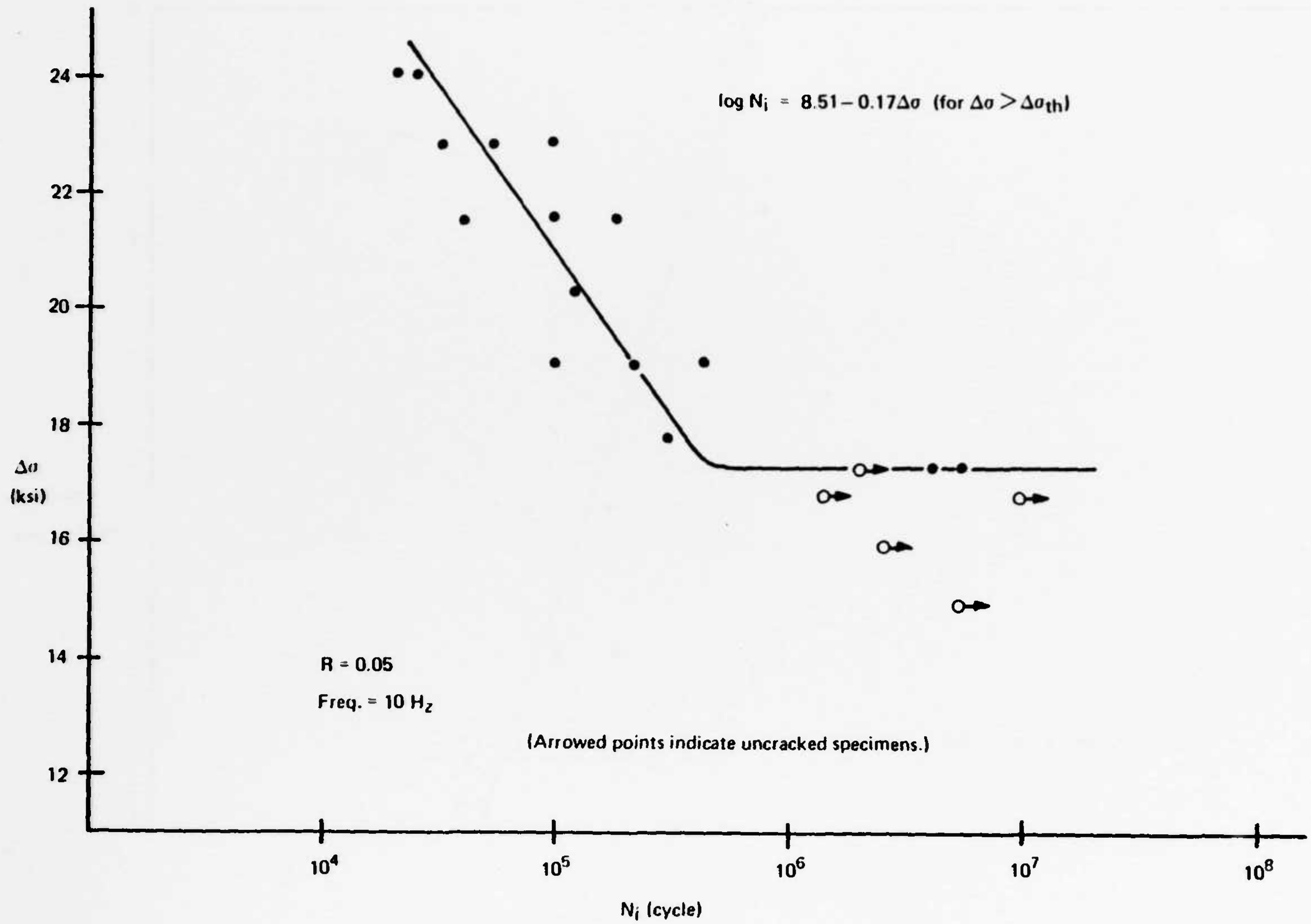

Figure 6. Variation of Fatigue Crack Initiation Life N_i with Stress Range $\Delta\sigma$

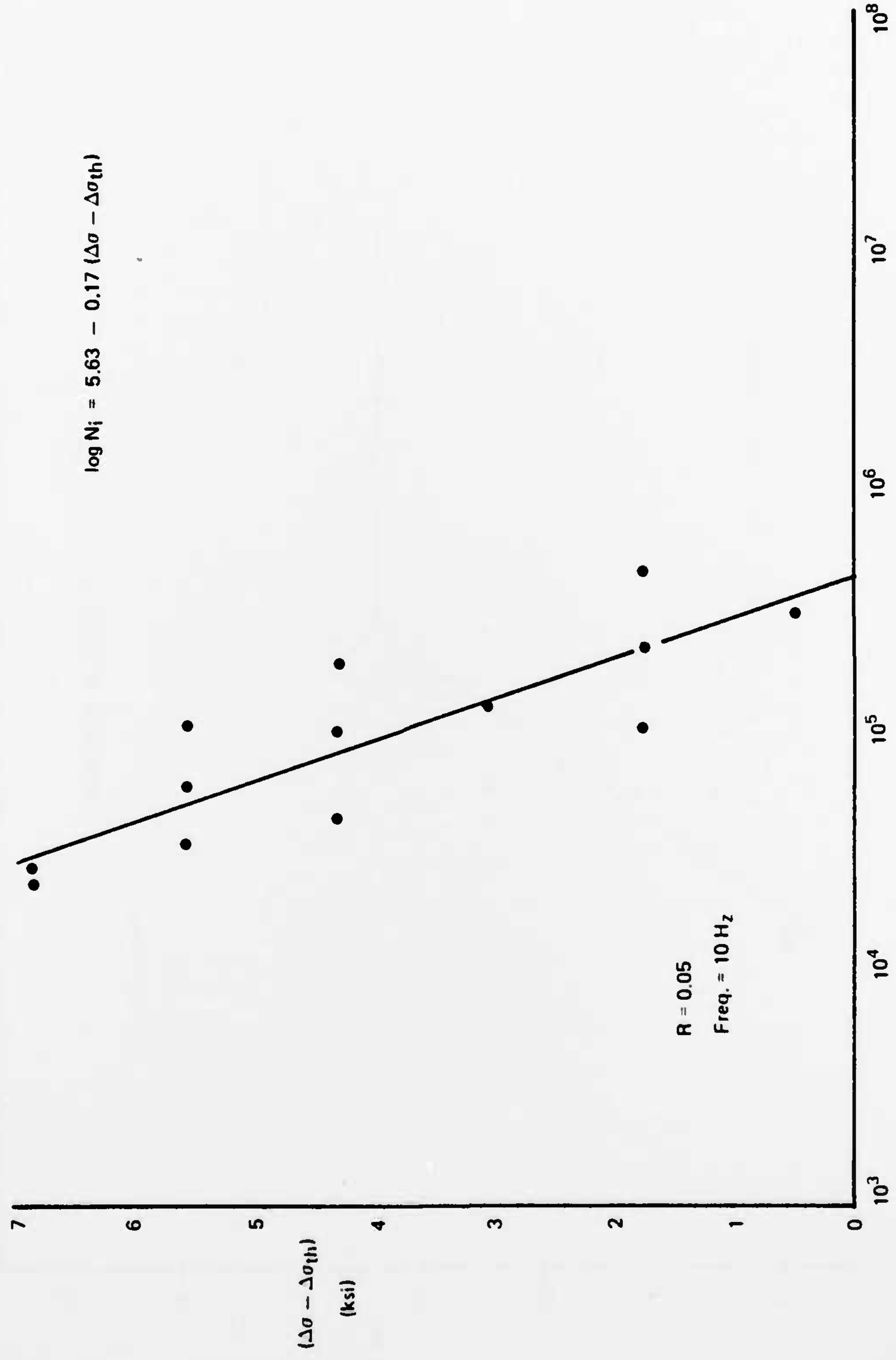

Figure 7. Variation of Fatigue Crack Initiation Life N_i with $(\Delta\sigma - \Delta\sigma_{th})$

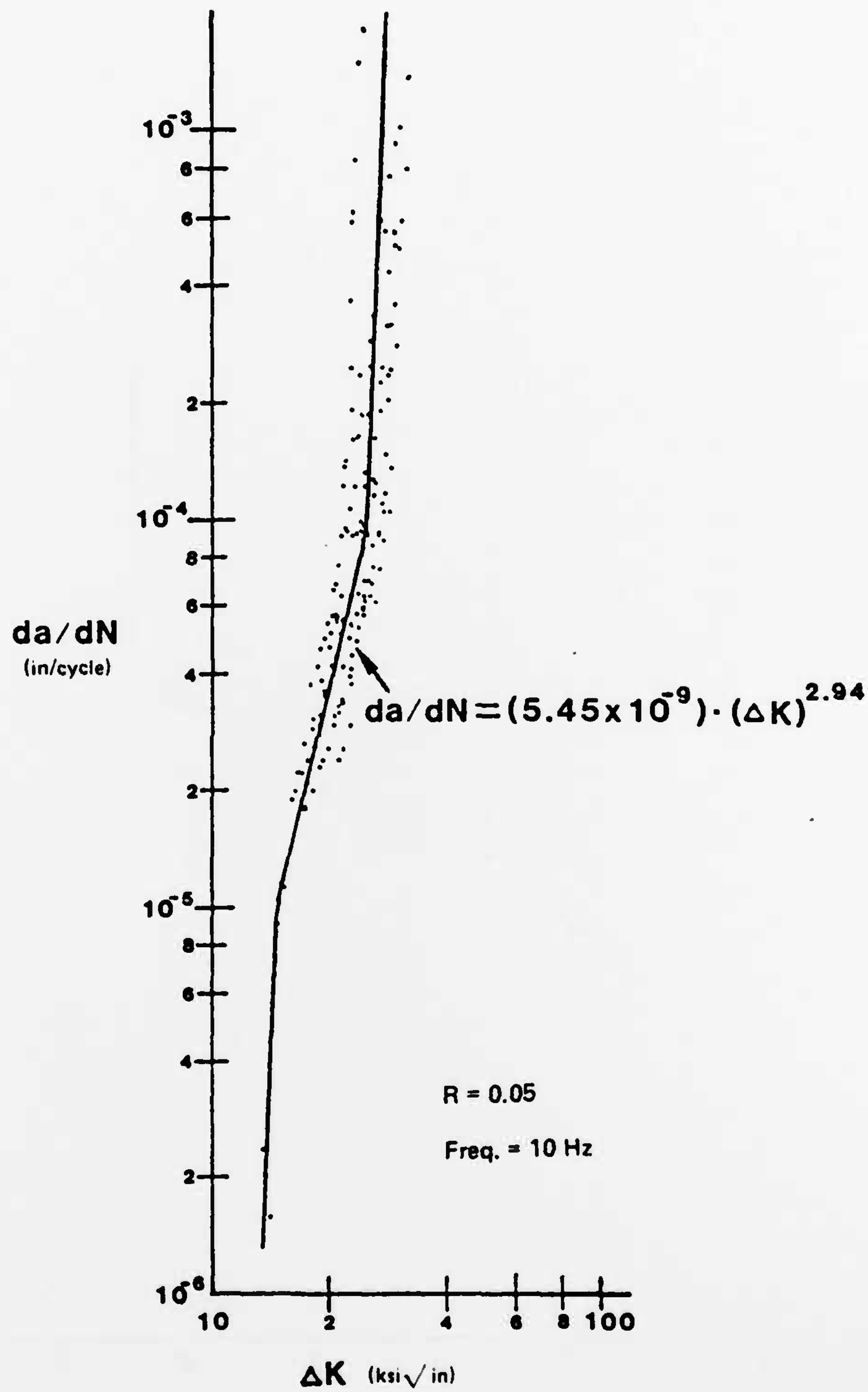

Figure 8. Variation of Fatigue Crack Growth Rate da/dN with Stress Intensity Factor Range ΔK

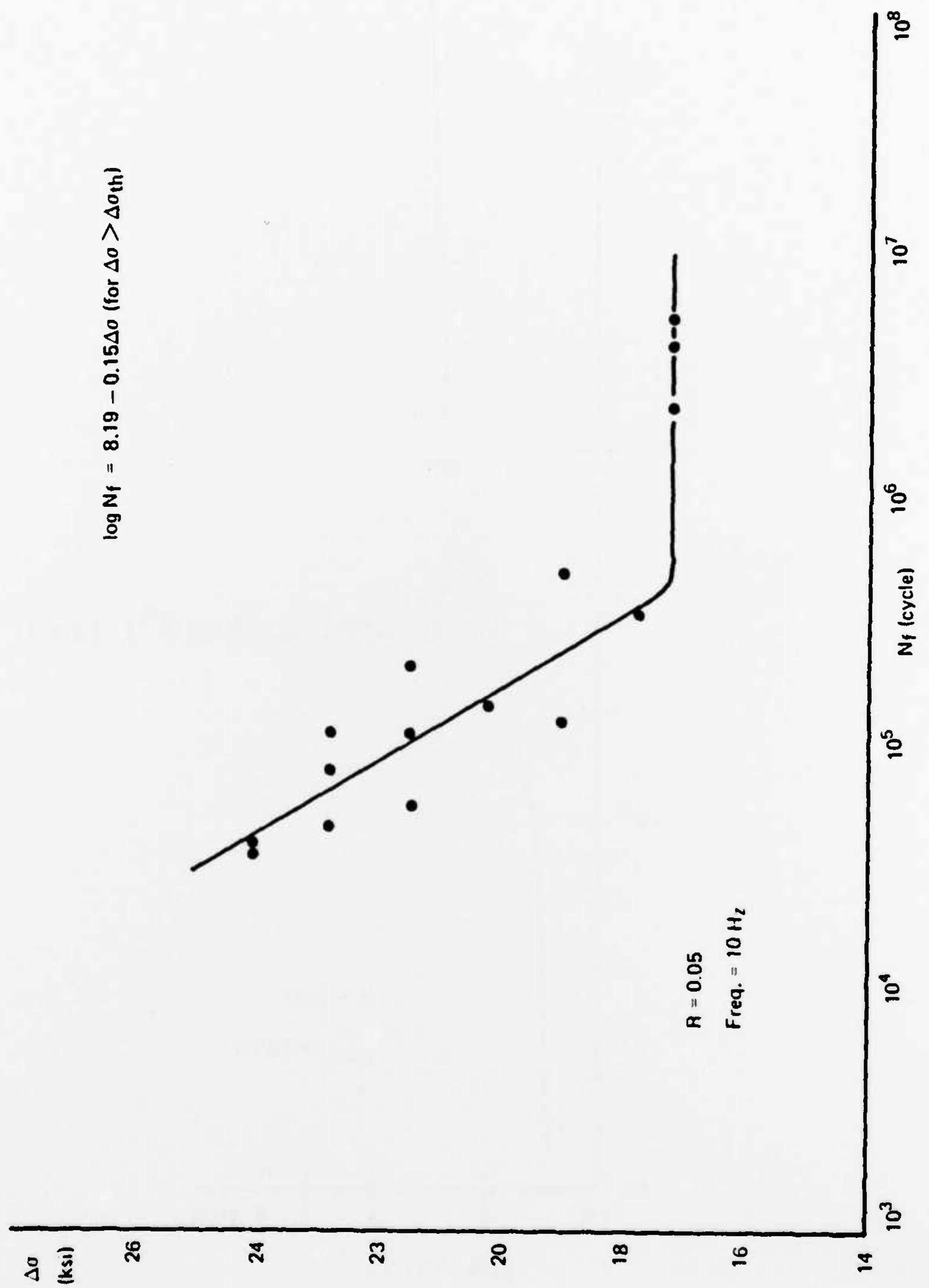

Figure 9. Variation of Total Fatigue Life N_f with Stress Range $\Delta\sigma$

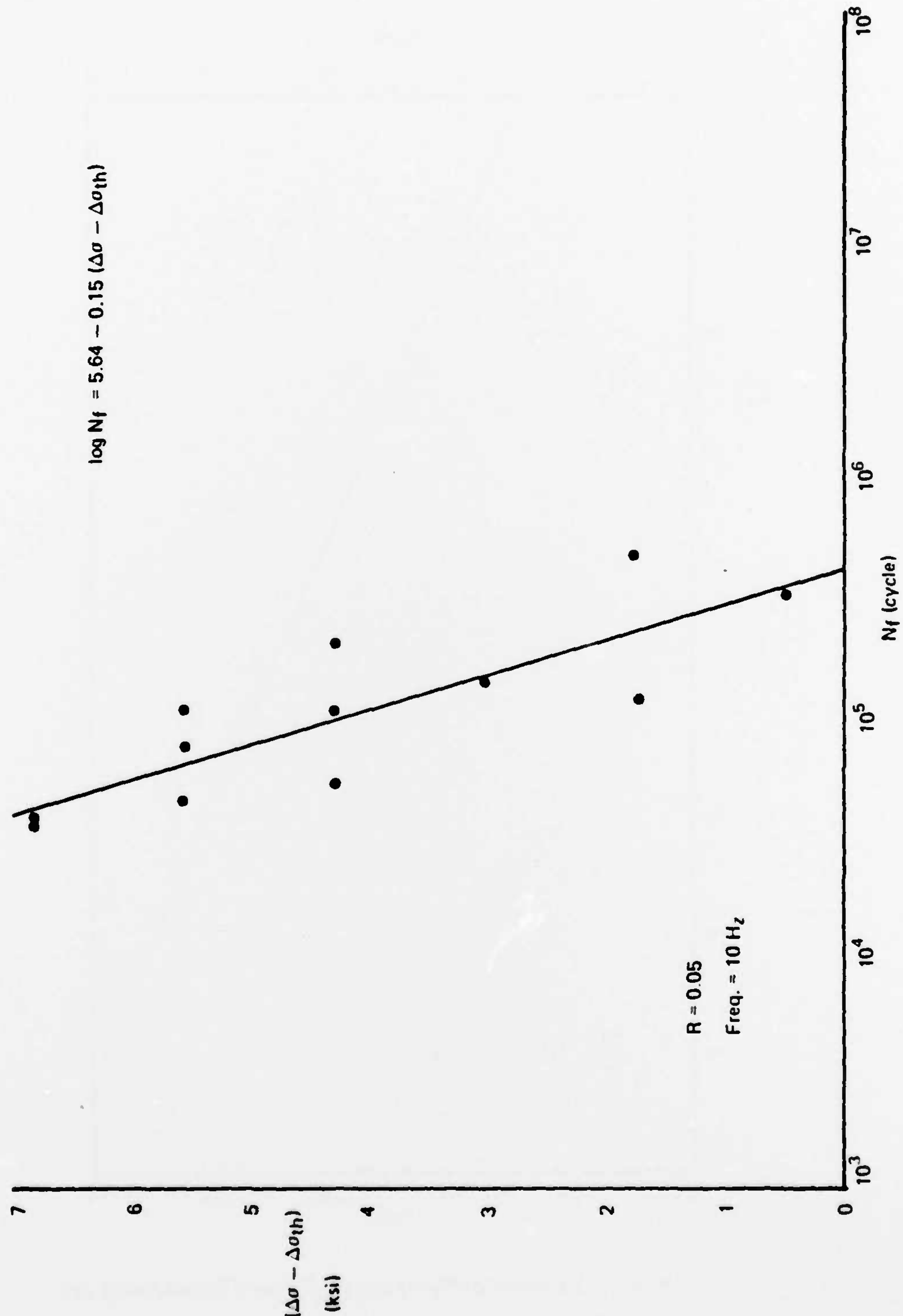

Figure 10. Variation of Total Fatigue Life N_f with $(\Delta\sigma - \Delta\sigma_{th})$

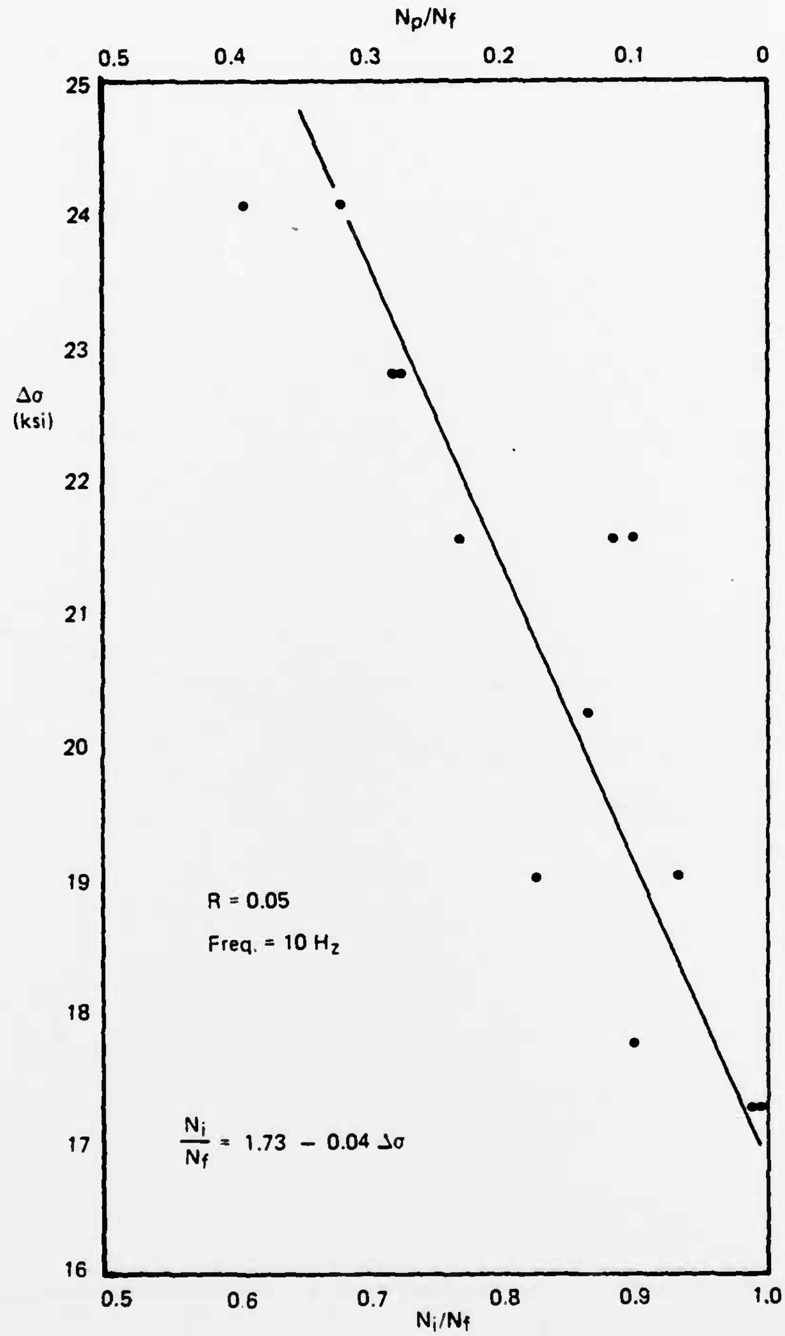

Figure 11. Variation of N_i/N_f and N_p/N_f with Stress Range $\Delta\sigma$

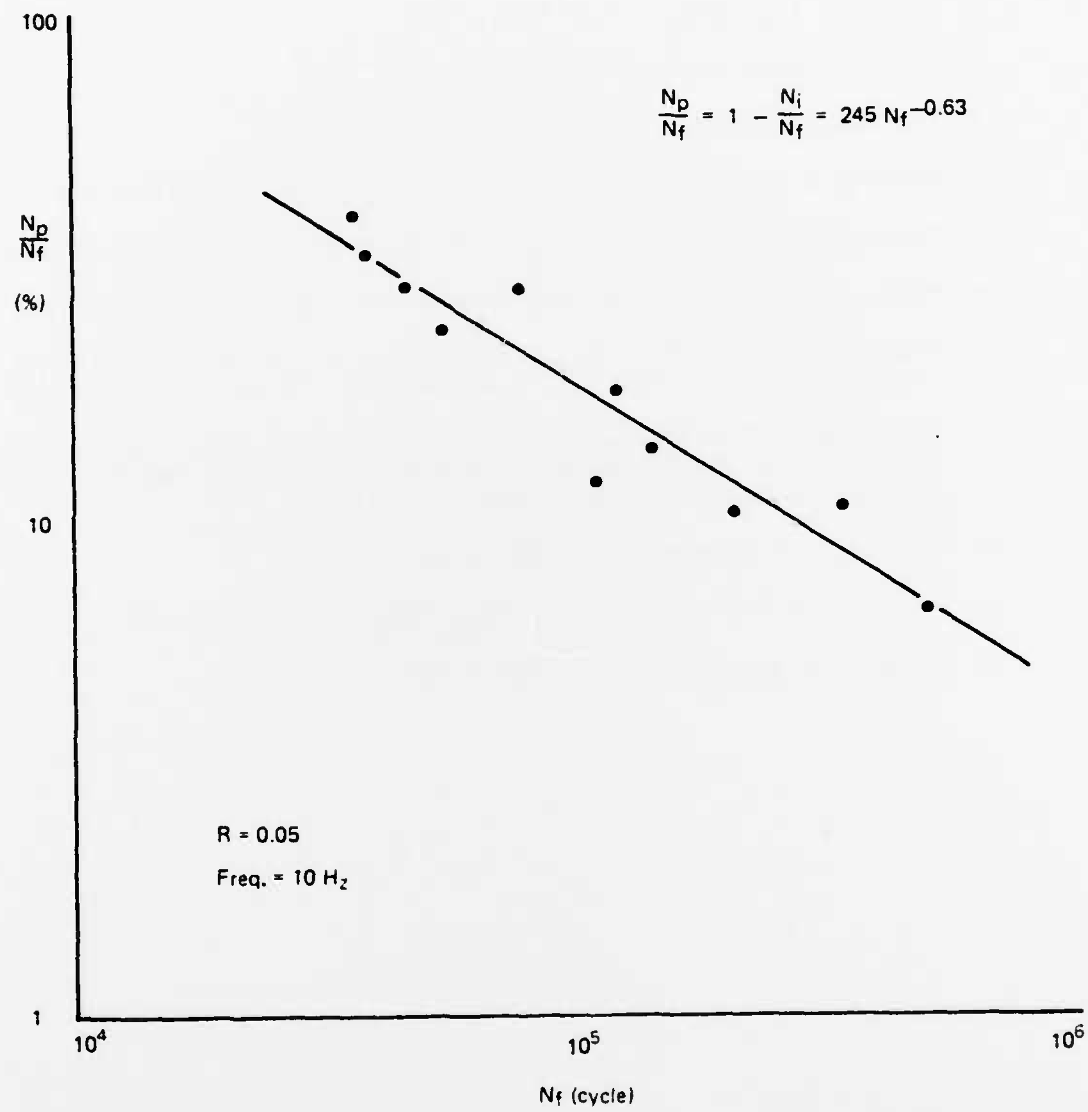

Figure 12. Variation of N_p/N_f with Total Fatigue Life N_f

REFERENCES

1. Forman, R. G., Eng. Fract. Mech., Vol. 4, 1972, p. 333.

2. Kim, Y. H., Private Communication.

3. Bowie, O L., J. Math. and Phys., Vol. 23, 1956, p. 60.

4. Isida, M., J. Appl. Mech., Vol. 33, 1966, p. 674.

5. Liu, A. F., Private Communication.

6. Paris, P. and Erdogan, F., J. Basic Eng., Vol. 85, 1963, p. 528.

7. Howland, R. C. J., Phil. Trans. Roy. Soc. (London), A, Vol. 229, 1929-30, p. 67.

8. Heywood, R.B., Designing by Photoelasticity, Chapman and Hall, London, 1952, p. 163.

9. Chanani, G. R., Northrop Corp. Report NOR-82-54, 1982.

10. Independent Research and Development Data Sheet, "Fatigue, Fracture Mechanics, and Damage Tolerant Structures," MDC Q0866-7, Vol. 2, McDonnell Aircraft Co., Feb. 28, 1983.

11. Margolis, W. S., "F-16 Material Test Allowables for Aluminum Alloy 7475, 3.0" Plate –T7351 Temper, and 0.5" Plate (92" Width) –T7651 Temper and –T7351 Temper," Report No. 16PR926, General Dynamics, April 1978.

12. Wetzel, R. M., J. Materials, Vol. 3, 1968, p. 646.

13. Allery, M. B. P. and Birkbeck, G., Eng. Fract. Mech., Vol. 4, 1972, p. 325.

14. Manson, S. S., Exp. Mech., Vol. 5, 1965, p. 193

DISTRIBUTION LIST

REPORT NO. NADC-83133-60

Work Unit GC12B/ZR00001

	No. of Copies
NAVAIRSYSCOM (AIR-0004)	9
2 for retention	
2 for AIR-530	
1 for AIR-320B	
1 for AIR-52032D	
1 for AIR-5302	
1 for AIR-53021	
1 for AIR-530215	
NAVSEASYCOM, Washington, D.C. 20362	1
NAVAIRTESTCEN, Patuxent River, Maryland	1
NAVAVNSAFECEN, NAS, Norfolk, Virginia	1
NAVSHIPRANDCEN, Bethesda, Maryland 20034	1
NAVSHIPRANDCEN, Annapolis, Maryland 21402	1
NRL, Washington, D. C. 20375	1
NAVAIREWORKFAC, NAS, Alameda (Code 340), California	1
Jacksonville (Code 340), Florida	1
Norfolk (Code 340), Virginia	1
North Island (Code 340), California	1
Pensacola (Code 340), Florida	1
MCAS, Cherry Point (Code 340), North Carolina	1
ONR, Washington, D.C. 20362	1
USAF Systems Command, WPAFB, Ohio 45433	
(Attn: FBR)	1
(Attn: FB)	1
(Attn: LLD)	1
(Attn: FYA)	1
(Attn: LAM)	1
(Attn: FBA)	1
(Attn: LPH)	1
DTIC	12
NAVAIRDEVCEN(8131)	3
NAVAIRDEVCEN(6043)	8

DAT
FILM